Available online at www.sciencedirect.com

ScienceDirect

www.elsevier.com/locate/brainres

Brain Research

Research Report

Resveratrol prevents akinesia and restores neuronal tyrosine hydroxylase immunoreactivity in the substantia *nigra pars* compacta of diabetic rats

Pamela Brambilla Bagatini[a,b], *Léder Leal Xavier*[c], *Laura Tartari Neves*[c], *Lisiani Saur*[c], *Sílvia Barbosa*[a], *Pedro Porto Alegre Baptista*[c], *Otávio Américo Augustin*[a], *Priscylla Nunes de Senna*[a,b], *Régis Gemerasca Mestriner*[c], *André Arigony Souto*[d], *Matilde Achaval*[a,b,*]

[a]*Laboratório de Histofisiologia Comparada, Departamento de Ciências Morfológicas, Instituto de Ciências Básicas da Saúde, Universidade Federal do Rio Grande do Sul, Avenida Sarmento Leite, 500, 90040-060 Porto Alegre, RS, Brazil*
[b]*Programa de Pós-Graduação em Neurociências, Universidade Federal do Rio Grande do Sul, Avenida Sarmento Leite, 500, 90040-060 Porto Alegre, RS, Brazil*
[c]*Laboratório de Biologia Celular e Tecidual, Departamento de Ciências Morfofisiológicas, Faculdade de Biociências, Pontifícia Universidade Católica do Rio Grande do Sul, Avenida Ipiranga, 6681, 90619-900 Porto Alegre, RS, Brazil*
[d]*Laboratório de Química de Produtos Naturais, Departamento de Química Pura, Faculdade de Química, Pontifícia Universidade Católica do Rio Grande do Sul, Avenida Ipiranga, 6681, 90619-900 Porto Alegre, RS, Brazil*

ARTICLE INFO

Article history:
Accepted 5 October 2014
Available online 22 October 2014

Keywords:
Diabetes
Resveratrol
Akinesia
Immunoreactivity
Tyrosine hydroxylase
Substantia *nigra pars* compacta

ABSTRACT

This study evaluated the effects of resveratrol on locomotor behaviors, neuronal and glial densities, and tyrosine hydroxylase immunoreactivity in the substantia *nigra pars* compacta of rats with streptozotocin-induced diabetes. Animals were divided into four groups: non-diabetic rats treated with saline (SAL), non-diabetic rats treated with resveratrol (RSV), diabetic rats treated with saline (DM) and diabetic rats treated with resveratrol (DM+RSV). The animals received oral gavage with resveratrol (20 mg/kg) for 35 days. The open field test and the bar test were performed to evaluate bradykinesia and akinesia, respectively. The Nissl-stained neuronal and glial densities and the dopaminergic neuronal density were estimated using planar morphometry. Tyrosine hydroxylase immunoreactivity was evaluated using regional and cellular optical densitometry. In relation to the locomotor behaviors, it was observed that the DM group developed akinesia, which was attenuated by resveratrol in the DM+RSV group, while the DM and DM+RSV groups showed bradykinesia. Our main morpho-physiological results demonstrated: a decrease in the cellular tyrosine hydroxylase immunoreactivity in the DM group, which was attenuated by resveratrol in

*Corresponding author at: Laboratório de Histofisiologia Comparada, Departamento de Ciências Morfológicas, Universidade Federal do Rio Grande do Sul (UFRGS), Avenida Sarmento Leite 500, Instituto de Ciências Básicas da Saúde, Sala 312, CEP 90050-170, Porto Alegre, RS, Brazil.

E-mail addresses: pamela.bagatini@yahoo.com.br (P.B. Bagatini), llxavier@pucrs.br (L.L. Xavier), laura.tartari@hotmail.com (L.T. Neves), lisi_saur@yahoo.com.br (L. Saur), slgentil@hotmail.com (S. Barbosa), pedropoa@gmail.com (P.P.A. Baptista), otavio_aa@yahoo.com.br (O.A. Augustin), priscyllasenna@hotmail.com (P.N. de Senna), regis.mestriner@pucrs.br (R.G. Mestriner), arigony@pucrs.br (A.A. Souto), machaval@pq.cnpq.br (M. Achaval).

http://dx.doi.org/10.1016/j.brainres.2014.10.007

the DM+RSV group; a higher neuronal density in the RSV group, when compared to the DM and DM+RSV groups; an increase in the glial density in the DM group, which was also reversed by resveratrol in the DM+RSV group. Resveratrol treatment prevents akinesia development and restores neuronal tyrosine hydroxylase immunoreactivity and glial density in the substantia *nigra pars* compacta of diabetic rats, suggesting that this polyphenol could be a potential therapeutic option against diabetes-induced nigrostriatal dysfunctions.

1. Introduction

Diabetes mellitus is a group of metabolic diseases characterized by hyperglycemia, which is increasingly seen as a public health burden worldwide (American Diabetes Association, 2012; Shaw et al., 2010). Chronic high blood glucose levels are related with the development of long-term dysfunctions and failure of various organs (Fowler, 2008). New evidence has emerged of the damage caused to the central nervous system and the cognitive deficits in diabetic patients with poor glycemic control (Biessels, 2013; Sima, 2010; Van Harten et al., 2006). Electrophysiological, neurochemical and structural brain abnormalities have been described in diabetic experimental models and in patients. Also, behavioral dysfunctions including psychomotor efficiency, motor speed and motor strength, have been observed (Biessels et al., 1994; Reagan, 2013; Roriz-Filho et al., 2009; Sims-Robinson et al., 2010).

In humans, studies suggest that diabetes has a potential impact on the development and/or the progression of Parkinson's disease (PD) (Cereda et al., 2013; Sun et al., 2012; Xu et al., 2011), a neurodegenerative disorder in dopaminergic neurons of the substantia *nigra pars* compacta (SNpc) which leads to reduced striatal dopamine levels and motor disabilities, such as akinesia, bradykinesia, resting tremor, and gait abnormalities (Dauer and Przedborski, 2003). Tyrosine hydroxylase (TH) is an important enzyme involved in dopamine production, catalyzing the conversion of the amino acid L-tyrosine to L-3,4-dihydroxyphenylalanine (L-DOPA), which is a rate-limiting step in the biosynthesis of dopamine (Nakashima et al., 2009). Streptozotocin (STZ)-induced diabetes has been shown to impair motor skills in rats, reducing the levels of RNAm for TH, as well as lowering the TH tissue content, mainly in the SNpc (Do Nascimento et al., 2011; Figlewicz et al., 1996).

There is a growing interest in the therapeutic potential of natural products to mitigate the negative effects of diabetes. Resveratrol (3,5,4′-trihydroxystilbene) is a polyphenol found in grapes and red wine, peanuts, different types of berries, and over 70 plant species (Harikumar and Aggarwal, 2008). This compound has been shown to exert pleiotropic effects on the modulation of various cell-signaling molecules and in the regulation of gene expression, which in turn can promote the expression of antioxidant enzymes, suppress the expression of inflammatory biomarkers, and modulate regulatory cell cycle genes (Baur and Sinclair, 2006; Harikumar and Aggarwal, 2008).

Interestingly, in STZ-induced diabetic rats, resveratrol has been shown to trigger beneficial effects in different brain areas by protecting against oxidative stress (Ates et al., 2007; Venturini et al., 2010), by ameliorating neurodegeneration and attenuating the expression of pro-inflammatory mediators and astrocytic activation in the hippocampus (Jing et al., 2013), and by preventing memory deficits (Schmatz et al., 2009). Furthermore, in PD rodent models, it has been demonstrated that treatment with resveratrol reduces motor disabilities and provides neuroprotection in the SNpc (Jin et al., 2008; Khan et al., 2010; Wang et al., 2011).

There is a lack of experimental evidence regarding the locomotor and neurohistological consequences of resveratrol treatment related to TH expression in the SNpc of diabetic rats. Thus, the goal of our study was to investigate the effects of oral treatment with resveratrol on locomotor behaviors, neuronal and glial densities, and regional and cellular TH immunoreactivity in the SNpc of rats with STZ-induced diabetes.

2. Results

A timeline with our experimental design can be seen in Fig. 1.

2.1. *Statistical power analysis*

The statistical power test is a helpful tool to calculate the minimum number of animals required to ensure reliable results. In the present study, the means and standard deviations from each parameter analyzed were used to estimate the statistical powers.

The findings of the statistical power analysis for body weight, blood glucose, bar test and open field evaluations were 100% for all these parameters. The findings for the density of the Nissl-stained neuronal and glial cells, density of TH immunoreactive neurons, and regional and cellular TH optical densitometries (ODs) were 97.5%, 93.4%, 95.1%, 99.7% and 99.9%, respectively.

The high statistical power values obtained in this evaluation confirms that the number of animals used in our experiments was adequate, and ensures the probability of statistical type II error is reduced. Thus, all the achieved results are reliable.

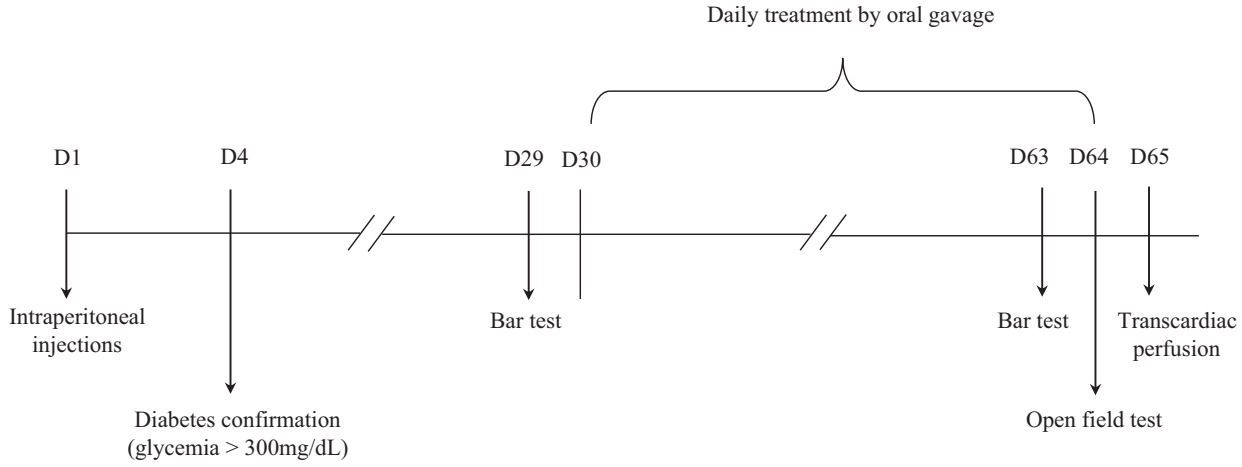

Fig. 1 – Timeline of the experimental design. D=day.

Table 1 – Body weight and blood glucose levels.

Groups	D1		D4		D30		D64	
	Weight (g)	Glycemia (mg/dL)	Weight (g)	Glycemia (mg/dL)	Weight (g)	Glycemia (mg/dL)	Weight (g)	Glycemia (mg/dL)
SAL	375.7±11.4	89.1±4.1	389.5±11.8	88±3.8	422.8±14.6	89.7±3.1	461.7±13.6	84.3±2.1
RSV	381.1±11.7	90.1±2.1	398.8±11.5	91.6±1.6	430.6±13.6	85.6±1.7	466.2±14.7	83.8±1.4
DM	368.2±4.9	86.5±3.2	328.7±6.9***	446.4±30.6***	307.8±8.9***	510.6±23.7***	299.8±7.7***	479.1±22.6***
DM+RSV	383.4±7.5	94.4±2.6	341.1±5.9[a,b]	377.6±21.2***	327.1±5.8***	501.7±25.2***	314.2±9.6***	484.9±24.9***

SAL: non-diabetic rats treated with saline, RSV: non-diabetic rats treated with resveratrol, DM: diabetic rats treated with saline, DM+RSV: diabetic rats treated with resveratrol. D: day.
*** Corresponds to $p<0.001$ compared to SAL and RSV groups.
[a] Corresponds to $p<0.01$ compared to SAL group.
[b] Corresponds to $p<0.001$ compared to RSV group.

2.2. *Body weight and blood glucose*

On day 1 (D1), there was no significant difference in body weight between the groups. On D4, the DM group presented a significant decrease in body weight compared to the SAL and RSV groups ($p<0.001$), likewise, the DM+RSV group presented a decrease when compared to the SAL ($p<0.01$) and RSV ($p<0.001$) groups. The body weight of diabetic rats from the DM and DM+RSV groups remained significantly lower on D30 and D64 ($p<0.001$) (Table 1).

Analysis of the glycemia data showed no differences in blood glucose levels between the groups on D1. From D4 onward, the blood glucose levels of rats from the DM and DM+RSV groups were significantly increased when compared to the SAL and RSV groups ($p<0.001$) (Table 1).

2.3. *Locomotor analyses*

2.3.1. *Bar test*

On D29, the time spent on the bar was not significantly different between the SAL (1.44±0.28), RSV (0.93±0.20), DM (1.67±0.23) and DM+RSV (1.52±0.16) groups (Fig. 2). On D63, rats from the DM group presented a significantly higher degree of akinesia (3.47±0.52) than the SAL (1.75±0.31; $p<0.05$), RSV (1.64±0.33; $p<0.01$) and DM+RSV (1.83±0.36; $p<0.05$) groups (Fig. 2).

2.3.2. *Open field test*

Analysis of the number of lines crossed in the open field test revealed that rats from the DM (35.25±4.58) and DM+RSV (35.18±15.23) groups crossed a significantly lower number of lines when compared to rats from the SAL (59.77±4.21; $p<0.05$) and RSV (63.15±7.46; $p<0.01$) groups (Fig. 3a).

The average speed in the DM group (0.02±0.00) was lower than in the SAL (0.03±0.00; $p<0.05$) and RSV (0.03±0.00; $p<0.01$) groups, with no significant difference compared to the DM+RSV group (0.02±0.00) (Fig. 3b).

No significant changes in maximum speed, time mobile and time immobile between groups were observed (data not shown).

2.4. *Histological and immunohistochemical analyses*

2.4.1. *Nissl-stained neuronal and glial density estimation*

The neuronal density was significantly reduced in the DM (2.51±0.21; $p<0.01$) and DM+RSV (2.98±0.30; $p<0.05$) groups when compared to the RSV group (5.10±0.69), while no such difference was observed in comparison to the SAL group (3.51±0.34) (Fig. 4a).

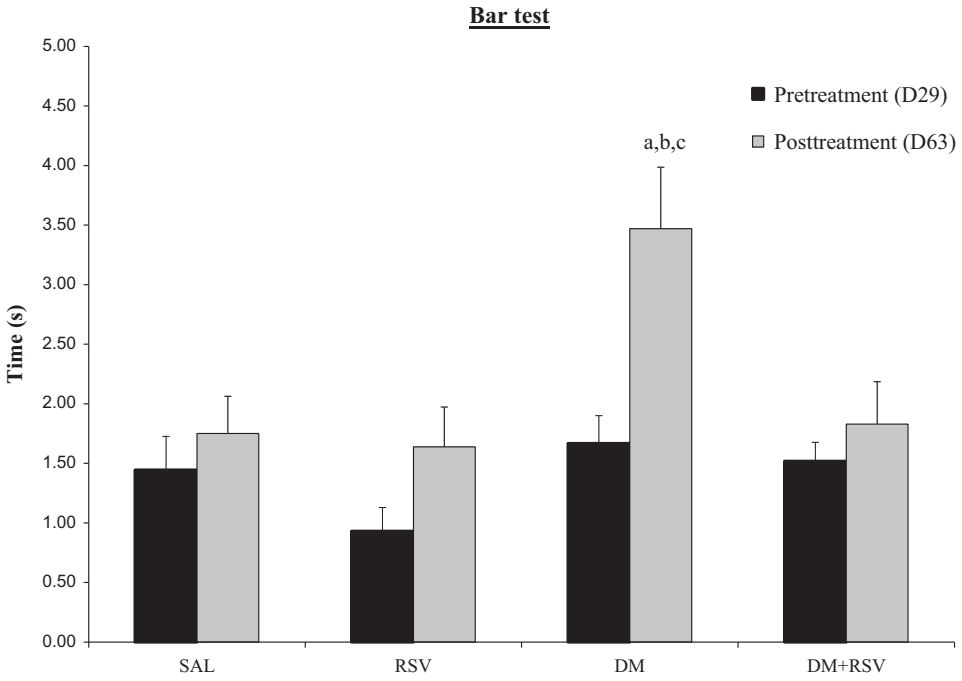

Fig. 2 – Latency to remove both paws from the horizontal bar in the bar test. [a]Corresponds to $p<0.05$ compared to the SAL group, [b]corresponds to $p<0.01$ compared to the RSV group, and [c] corresponds to $p<0.05$ compared to the DM+RSV group in posttreatment evaluation.

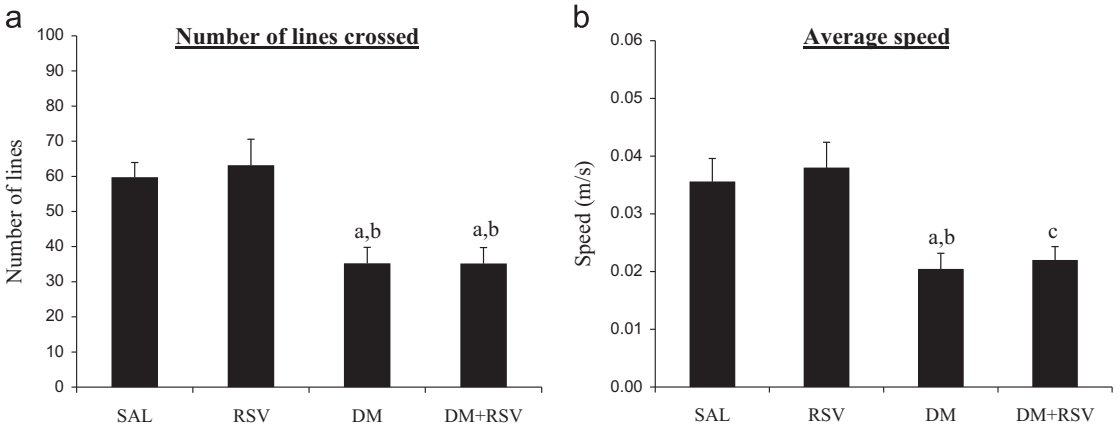

Fig. 3 – (a) Number of lines crossed in the open field test. [a]Corresponds to $p<0.05$ compared to the SAL group, and [b]corresponds to $p<0.01$ compared to the RSV group. (b) Average speed in the open field test. [a]Corresponds to $p<0.05$ compared to the SAL group, [b]corresponds to $p<0.01$ compared to the RSV group, and [c]corresponds to $p<0.05$ compared to the RSV group.

The glial density was significantly increased in the DM group (1.98±0.19) compared to the SAL (1.10±0.16) and DM+RSV (1.26±0.12) groups ($p<0.05$), with no significant difference when compared to the RSV group (1.59±0.13) (Fig. 4b).

Digitized images of Nissl-stained neuronal and glial cells in the SNpc of the experimental groups can be seen in Fig. 5.

2.4.2. *TH immunoreactive neuronal density estimation*

A significant reduction in TH immunoreactive neuronal density was only observed in the DM group (2.53±0.38) when compared to the RSV group (4.26±0.22; $p<0.05$), while no such difference was found in comparison with the SAL (3.63±0.30) and DM+RSV (3.33±0.18) groups (Fig. 6a).

2.4.3. *Optical densitometry*

Evaluation of regional OD demonstrated a reduction in TH immunoreactivity in the DM group (0.07±0.00) when compared to the RSV (0.11±0.00) and DM+RSV (0.11±0.00) groups ($p<0.05$), however, when compared to the SAL group, no difference was found (0.10±0.00) (Fig. 6b).

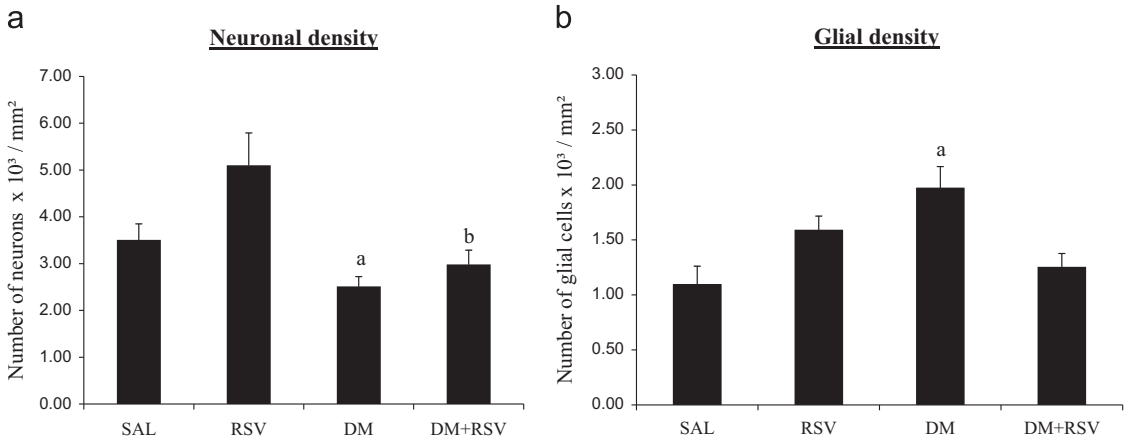

Fig. 4 – (a) Density of the Nissl-stained neurons in the SNpc. [a]corresponds to $p<0.01$ compared to the RSV group, and [b] corresponds to $p<0.05$ compared to the RSV group. (b) Density of the Nissl-stained glial cells in the SNpc. [a]corresponds to $p<0.05$ compared to the SAL and DM+RSV groups.

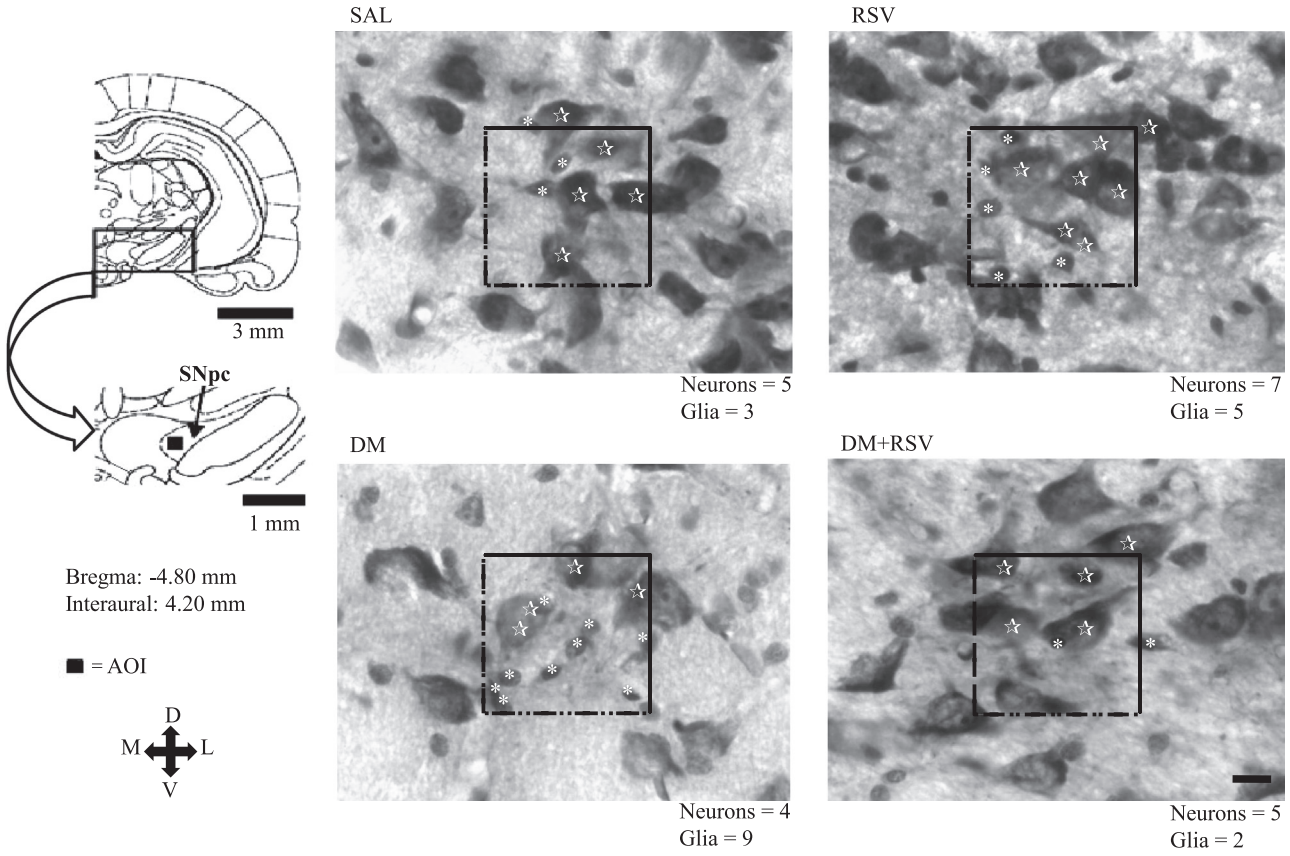

Fig. 5 – Digitized images from coronal mesencephalic sections, showing Nissl-stained neuronal and glial cells in the SNpc in the four experimental groups (SAL, RSV, DM and DM+RSV). Note the relative size of the area of interest (AOI) used to determine neuronal and glial densities. Neurons and glia located inside the AOI, or intersected by the upper and/or right edge of the AOI (continuous lines) were counted; neurons and glia that were intersected by the lower and/or left edge of the AOI (traced lines) were not counted. In the digitalized images, the stars (☆) depict neuronal cells, and the asterisks (*) depict glial cells; the total number of neurons and glia counted are presented in each image. The schemating drawings were modified from Paxinos and Watson (1998)'s atlas. Scale bar in the SNpc image: 10 μm.

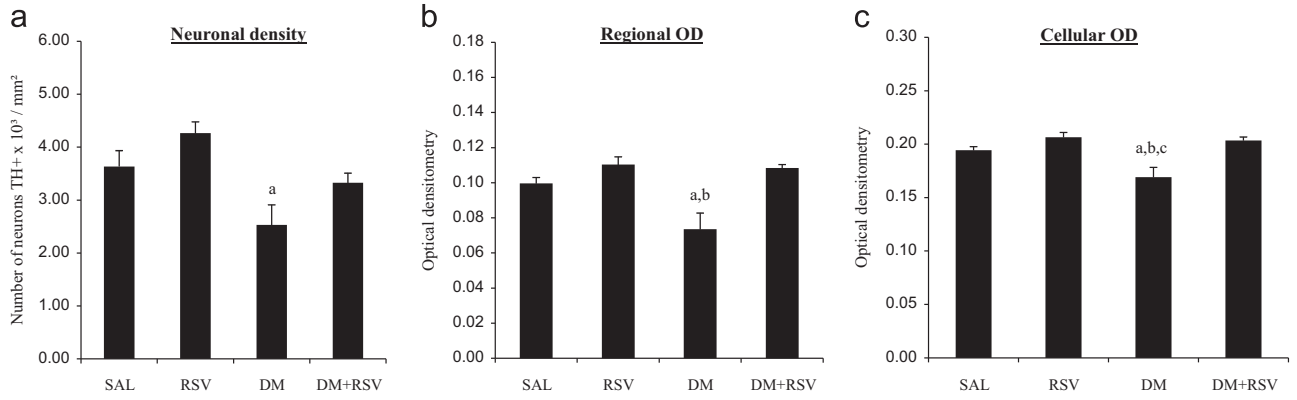

Fig. 6 – (a) Density of TH immunoreactive neurons in the SNpc. [a]Corresponds to $p<0.05$ compared to the RSV group. (b) Regional OD in the SNpc. [a]Corresponds to $p<0.05$ compared to the RSV group, and [b] corresponds to $p<0.05$ compared to the DM+RSV group. (c) Cellular OD in the SNpc. [a]Corresponds to $p<0.05$ compared to the SAL group, [b]corresponds to $p<0.01$ compared to the RSV group, and [c]corresponds to $p<0.01$ compared to the DM+RSV group.

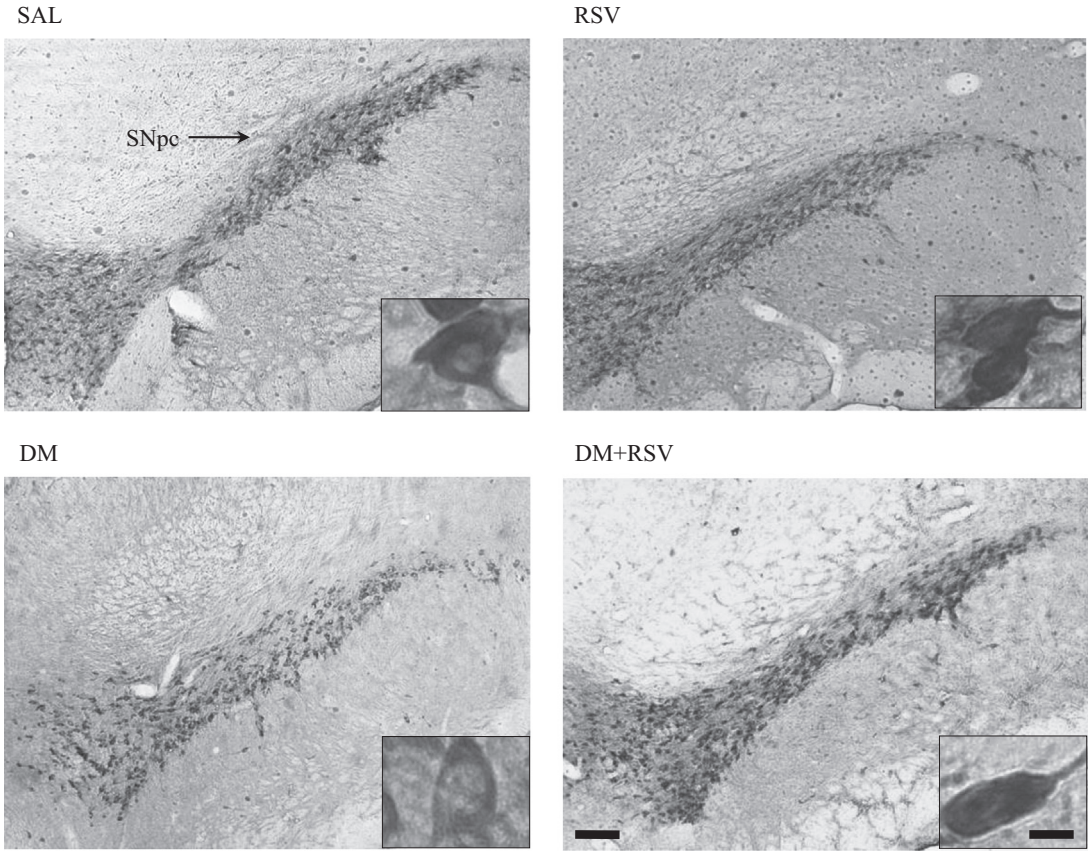

Fig. 7 – Digitized images from coronal mesencephalic sections, showing TH immunoreactivity in the SNpc in the four experimental groups (SAL, RSV, DM and DM+RSV). Images of the TH immunoreactive nigral neurons corresponding to each group are detailed in the lower left corner of the SNpc images. Note the reduced TH immunoreaction in the digitized image of the neuron from the DM group, compared to the SAL, RSV and DM+RSV groups. SNpc scale bar: 160 μm; neuron scale bar: 10 μm.

In cellular OD data analysis, the DM group presented a lower TH immunoreactivity in neuronal somata (0.17±0.00) when compared to the SAL (0.19±0.00; $p<0.05$), RSV (0.21±0.00; $p<0.01$) and DM+RSV (0.20±0.00; $p<0.01$) groups (Fig. 6c).

Digitized images of TH immunoreactivity in the SNpc of the experimental groups can be seen in Fig. 7.

3. Discussion

In diabetes, the primary cause of hyperglycemia is the deficient action of insulin on target tissues, which generates abnormalities in carbohydrate, lipid and protein metabolism. Uncontrolled high blood glucose levels triggers the classical

clinical symptoms of the disease, including marked polyuria, polydipsia and weight loss (American Diabetes Association, 2012). In the present study, these characteristics were observed in all the animals with STZ-induced diabetes and, as previous studies have shown, treatment with resveratrol was unable to influence the blood glucose levels and body weights of diabetic and non-diabetic rats (Ates et al., 2007; Kumar et al., 2007; Schmatz et al., 2009; Venturini et al., 2010).

Our experimental design demonstrated that STZ-induced diabetes can lead to two locomotor abnormalities which are hallmark symptoms of PD. Diabetic rats from the DM group presented a higher degree of akinesia in the bar test, and diabetic rats from both the DM and DM+RSV groups showed significant bradykinesia in the open field test, as shown by the decreased number of lines crossed and lower average speed. To the best of our knowledge, our study is the first to demonstrate akinesia development in diabetic rodents. Previous experimental evidences have demonstrated bradykinesia in rats with STZ-induced diabetes during the open field test (De Senna et al., 2011; Do Nascimento et al., 2011; Grzeda et al., 2007; Haider et al., 2013). In diabetic patients, psychomotor efficiency and motor speed are cognitive processes that can be negatively affected (Sims-Robinson et al., 2010), and the onset of diabetes prior to the development of PD is considered a risk factor for more severe Parkinsonian clinical symptoms (Cereda et al., 2012), suggesting that diabetes has a negative impact on nigrostriatal physiology.

Bradykinetic behaviors were not ameliorated by oral treatment with resveratrol. However, resveratrol was able to protect against akinesia development during the time course of the diabetes. This result demonstrates an unprecedented positive effect of resveratrol on this locomotor deficit, possibly due to its capability to attenuate some pathological mechanisms in brain regions responsible for motor control, such as the basal ganglia and cerebellum (Ates et al., 2007; Biessels et al., 1994; Cheema et al., 2011; Huang et al., 2012; Sima, 2010; Venturini et al., 2010).

Moreover, we demonstrated that diabetes leads to an increase in the density of Nissl-stained glial cells in the SNpc. The study by Wang et al. (2014) showed an increase in the number of microglial cells in the SNpc of diabetic mice. Therefore, the increased density of glial cells observed in our study may be the result of microglial reactivity.

On the other hand, the density of Nissl-stained neurons and TH immunoreactive neurons remained unaltered in the diabetic animals, when compared to the SAL group. Comparable to our findings, Wang et al. (2014) also showed no difference in the number of TH immunoreactive neurons in the SNpc of diabetic mice.

In addition, a decrease in cellular TH immunoreactivity was observed in diabetic rats, supporting the findings of the study from Do Nascimento et al. (2011) that showed a reduction in TH immunoreactivity in the SNpc of diabetic rats accompanied by bradykinesia in the open field test.

All these data suggest that microglia could act as an important factor in the dysfunctions seen in the SNpc of diabetic rodents, instigating inflammatory processes that might contribute to neurochemical impairments, such as the diminished cellular content of TH in nigral neurons (Hirsch and Hunot, 2009; Wang et al., 2014).

For the first time, our study showed that late starting (30 days) oral resveratrol treatment produces beneficial effects in the SNpc of diabetic rats by restoring glial density and cellular TH immunoreactivity. Other positive influences related to resveratrol treatment are that the RSV group presents increased Nissl-stained neuronal density when compared to the DM and DM+RSV groups, and the RSV and DM+RSV groups present increased regional TH immunoreactivity when compared to the DM group.

The SNpc is located in the ventral mesencephalon and is a constituent of the basal ganglia circuit. It receives inputs from the prefrontal cortex - striatum pathway, and projects dopaminergic outputs to the striatum (Dauer and Przedborski, 2003). Earlier studies demonstrated that diabetes is associated with a higher risk of PD development (Sun et al., 2012; Xu et al., 2011). Thus, the reduced TH neuronal content observed in our study could represent the beginning of a neurodegenerative process anteceded by microglial reactivity in the SNpc, as previously suggested (Halliday and Stevens, 2011; Wang et al., 2014). As well, the reduction in neuronal TH might lead to striatal dopamine deficiency and altered basal ganglia physiology, which in turn could lead to voluntary motor control impairment and development of classical PD symptoms in diabetic rats, such as akinesia and bradykinesia (Dauer and Przedborski, 2003).

In addition to the reduced TH content observed in nigral dopaminergic neurons, the alterations in motor behaviors found in the diabetic rats could have been incremented by peripheral neuropathy, low muscle mass and/or poor muscle strength (Andersen, 2012; Kalyani et al., 2014; Zangiabadi et al., 2011). As mentioned above, the open field test revealed dysfunctions in locomotor parameters in our diabetic groups. On the other hand, a cardinal feature of PD is difficulty initiating movement, which is evaluated by the bar test in rodents. Peripheral neuropathy and decreased muscle mass and strength could contribute to the development of akinesia in our diabetic model. However, the evidence from our study suggests the decreased cellular dopaminergic content in the SNpc is one of the main factors responsible for the development of akinesia, because this locomotor dysfunction was absent when this decrease was attenuated by resveratrol treatment in the DM+RSV group. It is important to remember that resveratrol was unable to reverse weight loss, which could have decreased muscle mass and strength in the DM+RSV group. This question might be better answered in future studies designed to assess the isolated effects of peripheral neuropathy, muscle mass and muscle strength in the akinesia degree, using the bar test.

The mechanisms involved in diabetes-induced nigrostriatal impairments are not well recognized. Hyperglycemia exerts neurotoxic effects by increasing the formation of reactive oxygen species (ROS) and advanced glycation end-products (AGEs), which enhance inflammatory responses and contribute to the development of microvascular brain pathology (Biessels, 2013; Roriz-Filho et al., 2009; Tomlinson and Gardiner, 2008). Furthermore, insulin is an important neurotrophic factor that regulates dopamine concentrations in the brain. In PD patients, a reduction was observed in the immunoreactivity and the expression of mRNA for insulin receptor in the substantia *nigra*, showing that insulin

deficiency possibly impairs neural plasticity in the SNpc (Craft and Watson, 2004; Roriz-Filho et al., 2009; Sima, 2010).

Oxidative stress and neuroinflammation are implicated in the pathophysiology of PD and diabetes-induced brain damages (Hirsch et al., 2012; Jenner, 2003; Sima, 2010; Wrighten et al., 2009). These mechanisms indicate that PD and diabetes possibly share common pathways that lead to glial changes and neuronal dysfunctions (Santiago and Potashkin, 2013).

Interestingly, the beneficial actions of resveratrol in the SNpc could be associated with multiple mechanisms. In cultured dopaminergic neurons, resveratrol was able to modulate the astroglial production of brain-derived neurotrophic factor (BDNF) and glial cell line-derived neurotrophic factor (GDNF), which are essential for neuronal and glial development, maintenance and survival (Zhang et al., 2012). In a model of lipopolysaccharide-induced neurotoxicity in midbrain neuron-glia cultures, resveratrol has been reported to protect dopaminergic neurons by reducing microglial reactivity and the generation of ROS and proinflammatory factors (Zhang et al., 2010). Resveratrol also provide neuroprotection in experimental models of PD and diabetes, by diminishing lipid peroxidation and the production of ROS, restoring the levels of antioxidant enzymes, and decreasing the content of proinflammatory cytokines (Ates et al., 2007; Jin et al., 2008; Jing et al., 2013; Khan et al., 2010; Lofrumento et al., 2014; Venturini et al., 2010).

Thus, the modulation of neurotrophic factors generation and redox status, and the antiinflammatory effects could explain the positive impact of resveratrol treatment on glial density and cellular TH immunoreactivity in the SNpc, and on the prevention of akinesia development in diabetic rats.

3.1. Conclusions

Our study demonstrated that experimental diabetes induced by STZ in rats can generate dysfunctions related to PD pathogenesis, such as akinesia, bradykinesia, increased glial density and reduced cellular TH immunoreactivity in the SNpc. Interestingly, on the 30th day following diabetes induction, beneficial effects were achieved by oral treatment with resveratrol, which was found to protect against akinesia, and to restore the glial density and the cellular TH immunoreactivity in the SNpc. Based on our results, we suggest that resveratrol might represent a relevant therapeutic option against diabetes-induced nigrostriatal dysfunctions. This is a novel finding and further investigation into this subject is required in experimental and clinical trials.

4. Experimental procedures

4.1. Chemicals

Streptozotocin (STZ), monoclonal antibody for tyrosine hydroxylase (TH) raised in mice, anti-mouse antibody conjugated with peroxidase, 3,3′-diaminobenzidine (DAB) and cresyl violet were obtained from Sigma Chemical Co. (USA). Thiopentax (sodium thiopental) was purchased from Cristalia (Brazil), and bovine serum albumin (BSA) from Inlab (Brazil). Isopentane and Entellan were obtained from Merck (Germany). *Trans*-resveratrol (*trans*-3,5,4′-trihydroxystilbene, extracted from *Polygonum cuspidatum*) was purchased from Chengdu Hawk Bio-Engineering (Beijing, China), and presented >99% of purity (confirmed by high performance liquid chromatography), as previously described (Souto et al., 2001). All other chemicals used were of analytical reagent grade.

4.2. Animals

Forty nine male *Wistar* rats obtained from the *Centro de Reprodução e Experimentação de Animais de Laboratório* (CREAL, *Universidade Federal do Rio Grande do Sul*–UFRGS), aged 12 weeks at the start of the experiment were used. Rats were housed in groups of three animals per cage. They were maintained under standard laboratory conditions, with free access to rat chow and water and a 12:12 light/dark cycle (lights on from 08:00 to 20:00 h). The experiments were conducted in accordance with the University guidelines, and were previously approved by the animal ethics committee of the University.

4.3. Experimental design

The animals were randomly divided into four groups, as follows: non-diabetic rats treated with saline (SAL), non-diabetic rats treated with resveratrol (RSV), diabetic rats treated with saline (DM) and diabetic rats treated with resveratrol (DM+RSV). For the bar test, 12 rats from the SAL group, 12 rats from the RSV group, 11 rats from the DM group and 9 rats from the DM+RSV group were analyzed. In the open field test, 13 rats from the SAL group, 13 rats from the RSV group, 12 rats from the DM group and 11 rats from the DM+RSV group were analyzed. Five rats per group were selected for histological and immunohistochemical procedures and analyses.

4.4. Experimental induction of diabetes

After an overnight fasting period (6 h), diabetes was induced by a single intraperitoneal (i.p.) injection of STZ (65 mg/kg of body weight) diluted in 0.1 M sodium-citrate buffer, pH 4.5. The non-diabetic rats received an equivalent amount of sodium-citrate buffer. 72 h after injections, blood glucose levels were measured in blood collected from the rat tail using a portable glucometer (On Call Plus, ACON Laboratories, USA). Only animals with blood glucose levels >300 mg/dL and symptoms of polyuria and polydipsia were considered diabetic and selected for the present study. During the experiment, the blood glucose levels of all the animals were verified at four moments: D1 (before i.p. injections of STZ and/or vehicle), D4 (72 h after i.p. injections), D30 and D64.

4.5. Oral treatment

From D30 to D64, oral treatment was provided to all groups once a day, between 10:00 and 11:00 a.m., totaling 35 days of treatment. Resveratrol was freshly dispersed in 0.9% saline solution and promptly administered via oral gavage to animals belonging to the RSV and DM+RSV groups, at a dose of

20 mg/kg of body weight, based on previous studies (Jin et al., 2008; Venturini et al., 2010; Wang et al., 2011). Animals from the SAL and DM groups received equal volumes of 0.9% saline solution alone. Resveratrol was stored at 5 °C in an amber flask, protected from light. The body weights of the animals were verified on D1, D4 and D30 and, in order to better control the resveratrol dose, from D30 to D64, they were verified twice a week (on Mondays and Thursdays).

4.6. Locomotor analyses

4.6.1. Bar test

The bar test was performed one day before the beginning of the treatment (D29) and one day before the last day of treatment (D63) to estimate the degree of akinesia at different time points of our experimental design. Akinesia was evaluated by gently placing both forelimbs on a 9 cm high horizontal bar, and the latency to remove both paws from the bar was measured in seconds. A cut-off time of 120 s was used as a maximum score (Amalric et al., 1986; Baptista et al., 2013).

4.6.2. Open field test

On D64, each rat were gently placed in a predetermined corner of a 50 cm × 40 cm × 60 cm box, in which the floor was divided into 12 equal squares, and the behavior was recorded for 3 min with a digital videocamera (DCR-SR47, Sony, Japan) (Carrera et al., 1998; Do Nascimento et al., 2011). ANY-maze software (version 4.70, Stoelting) was used to provide an automated analysis of distinct locomotor parameters: number of lines crossed, average speed, maximum speed, time mobile and time immobile.

The animals were submitted to a single open field test to avoid habituation to the open field apparatus, which could lead to decreased exploration and locomotion in response to repeated exposure to the task apparatus (Baptista et al., 2013; Leussis and Bolivar, 2006).

4.7. Histological and immunohistochemical procedures

At D65, the rats were anesthetized with sodium thiopental (50 mg/kg of body weight, i.p.) and perfused transcardially with 0.9% saline solution, followed by 4% paraformaldehyde (PF) in 0.1 M phosphate buffer (PB), pH 7.4. The brains were quickly removed from the skulls, postfixed in the 4% PF solution for 4 h at room temperature, and cryoprotected by immersion in a 15% and 30% sucrose solution in 0.1 M PB at 4 °C, until they sank. Finally, the brains were rapidly frozen in isopentane previously cooled in liquid nitrogen, and kept in a −80 °C freezer for further procedures.

The mesencephalic area that comprises the SNpc was identified between the following coordinates: interaural 4.2 mm, bregma −4.8 mm, and interaural 2.7 mm, bregma −6.3 mm (Paxinos and Watson, 1998). Coronal sections (30 μm thickness) from the SNpc were obtained from each brain using a cryostat (CM1850, Leica, Germany) at −20 °C and collected in PB saline (PBS), pH 7.4. Serial sections were selected to the Nissl staining method or TH immunohistochemistry.

4.7.1. Nissl staining

For the Nissl (cresyl violet) staining method, sections were mounted on gelatin-coated slides and air-dried. Thereafter, sections were rehydrated and stained with 0.02% cresyl violet in acetate buffer.

4.7.2. TH immunohistochemistry

The free-floating sections were pre-treated with 3% hydrogen peroxide in PBS for 30 min at room temperature, washed with PBS and blocked with 2% BSA in PBS containing 0.4% Triton X-100 (PBS-Tx) for 30 min. Thereafter, the sections were incubated with monoclonal TH antibody raised in mice, diluted 1:3000 in PBS-Tx for 48 h at 4 °C.

Subsequently, sections were washed in PBS-Tx and incubated with anti-mouse antibody conjugated with peroxidase diluted 1:500 in PBS-Tx for 2 h at room temperature. Sections were washed in PBS, and immunoreactivity was visualized by incubation in DAB and hydrogen peroxide.

Control sections were prepared by omitting the primary antibody and replacing it with PBS-Tx. In our study, all brains were fixed and post-fixed for the same time in identical solutions, carefully processed at the same time, and incubated in the same immunostaining medium for the same period of time. These precautions were performed to avoid overreaction, differences in chromogen reaction, saturation of OD or changes in background staining levels.

4.8. Histological and immunohistochemical analyses

4.8.1. Nissl-stained neuronal and glial density estimation

The number of neurons and glial cells per mm^2 of the SNpc was estimated by planar morphometry. The images were acquired using an Olympus BX50 optic microscope (Olympus, Japan) coupled to a digital camera (Opton, Brazil) and Image Pro Plus 6.0 software (Media Cybernetics, USA).

To estimate the neuronal and glial densities, five sections were selected from each rat. Six digitized images (40x) from medial, intermediary and lateral SNpc regions were obtained from each section (three images from the left and three images from the right brain hemispheres). Then, 30 images of the SNpc were analyzed per animal.

A square area of interest (AOI) measuring 597 μm^2 was overlaid on each image. Neurons and glial cells located inside the AOI, or intersected by the upper and/or right edge of the AOI were counted. Neurons and glial cells that were intersected by the lower and/or left edge of the AOI were not counted (Ferraz et al., 2008; Xavier et al., 2005).

The neurons were identified by their large and pale (euchromatic) nuclei surrounded by a violet stained cytoplasm. Glial cells were identified by the small and dark (heterochromatic) nuclei, and by the absence of stained cytoplasm. The nucleoli of neuronal cells and the nuclei of glial cells were considered as the counting markers for neurons and glia, respectively.

4.8.2. TH immunoreactive neuronal density estimation

The number of TH immunoreactive neurons per mm^2 of SNpc was estimated by planar morphometry. The images were acquired using an Axio Imager A1 optic microscope

(Zeiss, Germany) coupled to an AxioCam HRc camera (Zeiss, Germany), and Image Pro Plus 6.0 software.

For estimation of the TH immunoreactive neuronal density, five sections from each rat were selected. Six digitized images (40x) from medial, intermediary and lateral SNpc regions were obtained from each section (three images from the left and three images from the right brain hemispheres). Then, 30 images of the SNpc were analyzed per animal.

A square AOI measuring 784 μm^2 was overlaid on each image. The somata of the TH immunoreactive neurons located inside the AOI, or intersected by the upper and/or right edge of the AOI were counted. The somata that were intersected by the lower and/or left edge of the AOI were not counted (Ferraz et al., 2008; Xavier et al., 2005).

4.8.3. *Optical densitometry*

Semi-quantitative densitometric analyses were used to measure the intensity of TH immunoreactivity in the SNpc (Do Nascimento et al., 2011; Ferraz et al., 2008; Xavier et al., 2005). For these analyses, the same images and software from the TH immunoreactive neuronal density estimation section were used.

For the regional OD analysis, the digitized images were converted to an 8-bit gray scale (0–255 Gy levels) and an AOI measuring 784 μm^2 was overlaid on each image. Six OD measurements from each medial, intermediary and lateral SNpc regions were acquired per section, totalizing 30 OD measurements per animal.

For cellular OD analysis, the digitized images were also converted to an 8-bit gray scale (0–255 Gy levels), and one AOI measuring 3.7 μm^2 was placed over two different neuronal somata (avoiding the nucleus) in each image. Two somata OD measurements from each medial, intermediary and lateral SNpc regions were acquired per section, totalizing 60 OD measurements per animal.

All lighting conditions and magnifications were kept constant during the process of capturing the images. Background staining subtraction and correction were done in accordance with our previous published protocol (Xavier et al., 2005).

The OD was calculated using the following formula:

$$OD(x,y) = -\log\left[\frac{(INT(x,y) - BL)}{(INC - BL)}\right]$$

where "OD(x,y)" is the optical density at pixel(x,y), "INT(x,y)" or intensity is the intensity at pixel(x,y), "BL" or black is the intensity generated when no light goes through the material, and "INC" is the intensity of the incidental light.

4.9. *Statistical analyses*

The statistical analyses were carried out using SPSS 11.0 (Statistical Package for the Social Sciences, USA), and the G*Power 3 software (*Institut Für Experimentelle Psychologie*, *Heinrich Heine Universitat*, Germany) was used to calculate the statistical power (Faul et al., 2007). Data normality distribution was checked using the Kolmogorov-Smirnov test. Blood glucose, body weight and bar test data were analyzed using repeated measures analysis of variance (ANOVA), and differences between the groups were assessed using the Tukey *post hoc* test. Data from the open field test were analyzed using multivariate two-way ANOVA followed by the Tukey *post hoc* test. Histological and immunohistochemical data were analyzed using univariate two-way ANOVA followed by the Tukey *post hoc* test. Results are expressed as mean ± standard error of mean. $p < 0.05$ was considered significant.

Acknowledgments

This research was supported by grants from Conselho Nacional de Pesquisa e Desenvolvimento (CNPq), Coordenação de Aperfeiçoamento de Pessoal de Nível Superior (CAPES) and Fundação de Apoio à Pesquisa do Estado do Rio Grande do Sul (FAPERGS). Pamela Brambilla Bagatini was supported by a Ph. D. scholarship from CAPES. André Arigony Souto, Léder Leal Xavier and Matilde Achaval are CNPq investigators.

REFERENCES

Amalric, M., Blasco, T.A., Smith, N.T., Lee, D.E., Swerdlow, N.R., Koob, G.F., 1986. "Catatonia" produced by alfentanil is reversed by methylnaloxonium microinjections into the brain. Brain Res. 386 (1-2), 287–295, http://dx.doi.org/10.1016/0006-8993(86)90165-4.

American Diabetes Association, 2012. Diagnosis and classification of diabetes mellitus. Diabetes Care 35 (Suppl. 1), S64–S71, http://dx.doi.org/10.2337/dc12-s064.

Andersen, H., 2012. Motor dysfunction in diabetes. Diabetes/Metab. Res. Rev. 28 (Suppl. 1), 89–92, http://dx.doi.org/10.1002/dmrr.2257 (November 2011).

Ates, O., Cayli, S.R., Yucel, N., Altinoz, E., Kocak, A., Durak, M.A., Turkoz, Y., Yologlu, S., 2007. Central nervous system protection by resveratrol in streptozotocin-induced diabetic rats. J. Clin. Neurosci.: Official Journal of the Neurosurgical Society of Australasia 14 (3), 256–260, http://dx.doi.org/10.1016/j.jocn.2005.12.010.

Baptista, P.P.A., de Senna, P.N., Paim, M.F., Saur, L., Blank, M., do Nascimento, P., Ilha, J., Vianna, M.R.M., Mestriner, R., Xavier, L.L., 2013. Physical exercise down-regulated locomotor side effects induced by haloperidol treatment in Wistar rats. Pharmacol. Biochem. Behav., 104; 113–118, http://dx.doi.org/10.1016/j.pbb.2012.12.020.

Baur, J.A., Sinclair, D.A., 2006. Therapeutic potential of resveratrol: the in vivo evidence. Nat. Rev. Drug Discovery 5 (6), 493–506, http://dx.doi.org/10.1038/nrd2060.

Biessels, G.J., 2013. Sweet memories: 20 years of progress in research on cognitive functioning in diabetes. Eur. J. Pharmacol. 719 (1-3), 153–160, http://dx.doi.org/10.1016/j.ejphar.2013.04.055.

Biessels, G.J., Kappelle, A.C., Bravenboer, B., Erkelens, D.W., Gispen, W.H., 1994. Cerebral function in diabetes mellitus. Diabetologia 37, 643–650.

Carrera, M.P., Brunhara, F.C., Schwarting, R.K.W., Tomaz, C., 1998. Drug conditioning induced by intrastriatal apomorphine administration. Brain Res. 790 (1-2), 60, http://dx.doi.org/10.1016/S0006-8993(98)00047-X (6).

Cereda, E., Barichella, M., Cassani, E., Caccialanza, R., Pezzoli, G., 2012. Clinical features of Parkinson disease when onset of diabetes came first: a case-control study. Neurology 78 (19), 1507–1511, http://dx.doi.org/10.1212/WNL.0b013e3182553cc9.

Cereda, E., Barichella, M., Pedrolli, C., Klersy, C., Cassani, E., Caccialanza, R., Pezzoli, G., 2013. Diabetes and risk of Parkinson's disease. Mov. Disorders: Official Journal of the

Movement Disorder Society 28 (2), 257, http://dx.doi.org/10.1002/mds.25211.
Cheema, H., Federman, D., Kam, A., 2011. Hemichorea-hemiballismus in non-ketotic hyperglycaemia. J. Clin. Neurosci.: Official Journal of the Neurosurgical Society of Australasia 18 (2), 293–294, http://dx.doi.org/10.1016/j.jocn.2010.04.036.
Craft, S., Watson, G.S., 2004. Insulin and neurodegenerative disease: shared and specific mechanisms. Neurology 3, 169–178.
Dauer, W., Przedborski, S., 2003. Parkinson's disease: mechanisms and models. Neuron 39, 889–909, http://dx.doi.org/10.1016/S0896-6273(03)00568-3.
De Senna, P.N., Ilha, J., Baptista, P.P.A., do Nascimento, P.S., Leite, M.C., Paim, M.F., Gonçalves, C.A., Achaval, M., Xavier, L.L., 2011. Effects of physical exercise on spatial memory and astroglial alterations in the hippocampus of diabetic rats. Metab. Brain Dis. 26 (4), 269–279, http://dx.doi.org/10.1007/s11011-011-9262-x.
Do Nascimento, P.S., Lovatel, G.A., Barbosa, S., Ilha, J., Centenaro, L.A., Malysz, T., Xavier, L.L., Schaan, B.D., Achaval, M., 2011. Treadmill training improves motor skills and increases tyrosine hydroxylase immunoreactivity in the substantia nigra pars compacta in diabetic rats. Brain Res. 1382, 173–180, http://dx.doi.org/10.1016/j.brainres.2011.01.063.
Faul, F., Erdfelder, E., Lang, A., Buchner, A., 2007. G*Power 3: a flexible statistical power analysis program for the social, behavioral, and biomedical sciences. Behav. Res. Methods 39, 177–191, http://dx.doi.org/10.3758/BF03193146.
Ferraz, A.C., Matheussi, F., Szawka, R.E., Rizelio, V., Delattre, A.M., Rigon, P., Hermel, E.E.S., Xavier, L.L., Achaval, M., Anselmo-Franci, J.A., 2008. Evaluation of estrogen neuroprotective effect on nigrostriatal dopaminergic neurons following 6-hydroxydopamine injection into the substantia nigra pars compacta or the medial forebrain bundle. Neurochem. Res. 33 (7), 1238–1246, http://dx.doi.org/10.1007/s11064-007-9575-7.
Figlewicz, D., Brot, M., McCall, A., Szot, P., 1996. Diabetes causes differential changes in CNS noradrenergic and dopaminergic neurons in the rat: a molecular study. Brain Res. 736, 54–60.
Fowler, M.J., 2008. Microvascular and macrovascular complications of diabetes. Clin. Diabetes 26 (2), 77–82, http://dx.doi.org/10.2337/diaclin.26.2.77.
Grzeda, E., Wiśniewska, R.J., Wiśniewski, K., 2007. Effect of an NMDA receptor agonist on T-maze and passive avoidance test in 12-week streptozotocin-induced diabetic rats. Pharmacol. Rep. 59 (6), 656–663 (Retrieved from) ⟨http://www.ncbi.nlm.nih.gov/pubmed/18195454⟩.
Haider, S., Ahmed, S., Tabassum, S., Memon, Z., Ikram, M., Haleem, D.J., 2013. Streptozotocin-induced insulin deficiency leads to development of behavioral deficits in rats. Acta Neurol. Belg. 113 (1), 35–41, http://dx.doi.org/10.1007/s13760-012-0121-2.
Halliday, G.M., Stevens, C.H., 2011. Glia: initiators and progressors of pathology in Parkinson's disease. Mov. Disorders 26 (1), 6–17, http://dx.doi.org/10.1002/23455.
Harikumar, K.B., Aggarwal, B.B., 2008. Resveratrol: a multitargeted agent for age-associated chronic diseases. Cell Cycle 7, 1020–1035, http://dx.doi.org/10.4161/cc.7.8.5740 (April).
Hirsch, E.C., Hunot, S., 2009. Neuroinflammation in Parkinson's disease: a target for neuroprotection?. Lancet Neurol. 8 (4), 382–397, http://dx.doi.org/10.1016/S1474-4422(09)70062-6.
Hirsch, E.C., Vyas, S., Hunot, S., 2012. Neuroinflammation in Parkinson's disease. Parkinsonism Relat. Disorders 18 (Suppl 1), S210, http://dx.doi.org/10.1016/S1353-8020(11)70065-7 (2).
Huang, M., Gao, L., Yang, L., Lin, F., Lei, H., 2012. Abnormalities in the brain of streptozotocin-induced type 1 diabetic rats revealed by diffusion tensor imaging. NeuroImage Clin. 1 (1), 57–65, http://dx.doi.org/10.1016/j.nicl.2012.09.004.
Jenner, P., 2003. Oxidative stress in Parkinson's disease. Ann. Neurol. 53 (Suppl. 3)http://dx.doi.org/10.1002/ana.10483 (S26–36; discussion S36–8).
Jin, F., Wu, Q., Lu, Y.-F., Gong, Q.-H., Shi, J.-S., 2008. Neuroprotective effect of resveratrol on 6-OHDA-induced Parkinson's disease in rats. Eur. J. Pharmacol. 600 (1-3), 78–82, http://dx.doi.org/10.1016/j.ejphar.2008.10.005.
Jing, Y.-H., Chen, K.-H., Kuo, P.-C., Pao, C.-C., Chen, J.-K., 2013. Neurodegeneration in streptozotocin-induced diabetic rats is attenuated by treatment with resveratrol. Neuroendocrinology 98 (2), 116–127, http://dx.doi.org/10.1159/000350435.
Kalyani, R.R., Corriere, M., Ferrucci, L., 2014. Age-related and disease-related muscle loss: the effect of diabetes, obesity, and other diseases. Lancet Diabetes Endocrinol. 2 (10), 819–829, http://dx.doi.org/10.1016/S2213-8587(14)70034-8.
Khan, M.M., Ahmad, A., Ishrat, T., Khan, M.B., Hoda, M.N., Khuwaja, G., Raza, S.S., Khan, A., Javed, H., Vaibhav, K., Islam, F., 2010. Resveratrol attenuates 6-hydroxydopamine-induced oxidative damage and dopamine depletion in rat model of Parkinson's disease. Brain Res. 1328, 139–151, http://dx.doi.org/10.1016/j.brainres.2010.02.031.
Kumar, A., Kaundal, R.K., Iyer, S., Sharma, S.S., 2007. Effects of resveratrol on nerve functions, oxidative stress and DNA fragmentation in experimental diabetic neuropathy. Life Sci. 80 (13), 1236–1244, http://dx.doi.org/10.1016/j.lfs.2006.12.036.
Leussis, M.P., Bolivar, V.J., 2006. Habituation in rodents: a review of behavior, neurobiology, and genetics. Neurosci. Biobehav. Rev. 30 (7), 1045–1064, http://dx.doi.org/10.1016/j.neubiorev.2006.03.006.
Lofrumento, D.D., Nicolardi, G., Cianciulli, A., De Nuccio, F., La Pesa, V., Carofiglio, V., Dragone, T., Calvello, R., Panaro, M.A., 2014. Neuroprotective effects of resveratrol in an MPTP mouse model of Parkinson's-like disease: Possible role of SOCS-1 in reducing pro-inflammatory responses. Innate Immu. 20 (3), 249–260, http://dx.doi.org/10.1177/1753425913488429.
Nakashima, A., Hayashi, N., Kaneko, Y.S., Mori, K., Sabban, E.L., Nagatsu, T., Ota, A., 2009. Role of N-terminus of tyrosine hydroxylase in the biosynthesis of catecholamines. J. Neural Transm. (Vienna, Austria: 1996) 116 (11), 1355–1362, http://dx.doi.org/10.1007/s00702-009-0227-8.
Paxinos, G., Watson, C., 1998. The Rat Brain in Stereotaxic Coordinates. Academic Press, San Diego.
Reagan, L.P., 2013. Diabetes as a chronic metabolic stressor: causes, consequences and clinical complications. Exp. Neurol. 233 (1), 68–78, http://dx.doi.org/10.1016/j.expneurol.2011.02.004.DIABETES.
Roriz-Filho, J., Sá-Roriz, T.M., Rosset, I., Camozzato, A.L., Santos, A.C., Chaves, M.L.F., Moriguti, J.C., Roriz-Cruz, M., 2009. (Pre) diabetes, brain aging, and cognition. Biochim. Biophys. Acta 1792 (5), 432–443, http://dx.doi.org/10.1016/j.bbadis.2008.12.003.
Santiago, J.A., Potashkin, J.A., 2013. Shared dysregulated pathways lead to Parkinson's disease and diabetes. Trends Mol. Med. 19 (3), 176–186, http://dx.doi.org/10.1016/j.molmed.2013.01.002.
Schmatz, R., Mazzanti, C.M., Spanevello, R., Stefanello, N., Gutierres, J., Corrêa, M., da Rosa, M.M., Rubin, M.A., Schetinger, M., R., C, Morsch, V.M., 2009. Resveratrol prevents memory deficits and the increase in acetylcholinesterase activity in streptozotocin-induced diabetic rats. Eur. J. Pharmacol. 610 (1-3), 42, http://dx.doi.org/10.1016/j.ejphar.2009.03.032 (8).
Shaw, J.E., Sicree, R.A., Zimmet, P.Z., 2010. Global estimates of the prevalence of diabetes for 2010 and 2030. Diabetes Res. Clin. Pract. 87 (1), 4–14, http://dx.doi.org/10.1016/j.diabres.2009.10.007.

Sima, A.A.F., 2010. Encephalopathies: the emerging diabetic complications. Acta Diabetol. 47 (4), 279–293, http://dx.doi.org/10.1007/s00592-010-0218-0.

Sims-Robinson, C., Kim, B., Rosko, A., Feldman, E.L., 2010. How does diabetes accelerate Alzheimer disease pathology? Nat. Rev. Neurol. 6 (10), 551–559, http://dx.doi.org/10.1038/nrneurol.2010.130.

Souto, A.A., Carneiro, M.C., Seferin, M., Senna, M.J.H., Conz, A., Gobbi, K., 2001. Determination of trans-resveratrol concentrations in Brazilian Red Wines by HPLC. J. Food Compos. Anal. 14 (4), 441–445, http://dx.doi.org/10.1006/jfca.2000.0970.

Sun, Y., Chang, Y.-H., Chen, H.-F., Su, Y.-H., Su, H.-F., Li, C.-Y., 2012. Risk of Parkinson disease onset in patients with diabetes: a 9-year population-based cohort study with age and sex stratifications. Diabetes Care 35 (5), 1047–1049, http://dx.doi.org/10.2337/dc11-1511.

Tomlinson, D.R., Gardiner, N.J., 2008. Glucose neurotoxicity. Nat. Rev. Neurosci. 9 (1), 36–45, http://dx.doi.org/10.1038/nrn2294.

Van Harten, B., de Leeuw, F., Weinstein, H., Scheltens, P., Biessels, G., 2006. Brain imaging in patients with diabetes. Diabetes Care 29 (11), 2539–2548, http://dx.doi.org/10.2337/dc-06-1637.

Venturini, C.D., Merlo, S., Souto, A.A., Fernandes, M.D.C., Gomez, R., Rhoden, C.R., 2010. Resveratrol and red wine function as antioxidants in the nervous system without cellular proliferative effects during experimental diabetes. Oxidative Med. Cell. Longevity 3 (6), 434–441, http://dx.doi.org/10.4161/oxim.3.6.14741.

Wang, L., Zhai, Y.-Q., Xu, L.-L., Qiao, C., Sun, X.-L., Ding, J.-H., Lu, M., Hu, G., 2014. Metabolic inflammation exacerbates dopaminergic neuronal degeneration in response to acute MPTP challenge in type 2 diabetes mice. Exp. Neurol. 251, 22–29, http://dx.doi.org/10.1016/j.expneurol.2013.11.001.

Wang, Y., Xu, H., Fu, Q., Ma, R., Xiang, J., 2011. Protective effect of resveratrol derived from Polygonum cuspidatum and its liposomal form on nigral cells in parkinsonian rats. J. Neurol. Sci. 304 (1-2), 29–34, http://dx.doi.org/10.1016/j.jns.2011.02.025.

Wrighten, S.A., Piroli, G.G., Grillo, C.A., Reagan, L.P., 2009. A look inside the diabetic brain: contributors to diabetes-induced brain aging. Biochim. Biophys. Acta 1792 (5), 444–453, http://dx.doi.org/10.1016/j.bbadis.2008.10.013.

Xavier, L.L., Viola, G.G., Ferraz, A.C., Da Cunha, C., Deonizio, J.M. D., Netto, C.A., Achaval, M., 2005. A simple and fast densitometric method for the analysis of tyrosine hydroxylase immunoreactivity in the substantia nigra pars compacta and in the ventral tegmental area. Brain Res. Brain Res. Rev. 16 (1-3), 58–64, http://dx.doi.org/10.1016/j.brainresprot.2005.10.002.

Xu, Q., Park, Y., Huang, X., Hollenbeck, A., Blair, A., Schatzkin, A., Chen, H., 2011. Diabetes and risk of Parkinson's disease. Diabetes Care 34 (4), 910–915, http://dx.doi.org/10.2337/dc10-1922.

Zangiabadi, N., Asadi-Shekaari, M., Sheibani, V., Jafari, M., Shabani, M., Asadi, A.R., Tajadini, H., Jarahi, M., 2011. Date fruit extract is a neuroprotective agent in diabetic peripheral neuropathy in streptozotocin-induced diabetic rats: a multimodal analysis. Oxidative Med. Cell. Longevity 2011, 976948, http://dx.doi.org/10.1155/2011/976948.

Zhang, F., Shi, J.-S., Zhou, H., Wilson, B., Hong, J.-S., Gao, H.-M., 2010. Resveratrol protects dopamine neurons against lipopolysaccharide-induced neurotoxicity through its anti-inflammatory actions. Mol. Pharmacol. 78 (3), 466–477, http://dx.doi.org/10.1124/mol.110.064535.

Zhang, F., Wang, Y.-Y., Liu, H., Lu, Y.-F., Wu, Q., Liu, J., Shi, J.-S., 2012. Resveratrol produces neurotrophic effects on cultured dopaminergic neurons through prompting astroglial BDNF and GDNF release. Evidence-Based Complement. Altern. Med.: eCAM 2012, 937605, http://dx.doi.org/10.1155/2012/937605.